Analysis and application of a fractional SIR model constructed with Mittag-Leffler distribution

Noemi Zeraick Monteiro[1], Sandro Rodrigues Mazorche[1]

[1]*Dept. of Mathematics, Federal University of Juiz de Fora*
Juiz de Fora, 36036-900, Minas Gerais, Brazil
nzmonteiro@ice.ufjf.br, sandro.mazorche@ufjf.edu.br

Abstract. We have discussed previously the construction of an arbitrary-order SIR model with physical meaning. We believe that arbitrary-order derivatives can be obtained through potential laws in the infectivity and removal functions. This work intends to complete previous discussions, showing new results in a model with Mittag-Leffler distribution, with an emphasis on equilibrium points and reproduction numbers. We also discuss our prior application to COVID-19, now from the current perspective.

Keywords: SIR model, Arbitrary-order derivatives, Mittag-Leffler, COVID-19

1 Introduction

Fractional modeling allows capturing the dependence of previous stages on materials or processes and, as such, can bring biological, rheological, mechanical and electrical systems closer to reality. In particular, compartmental models have been widely studied with arbitrary orders (e.g. [1]; [2]).

In our work, we are interested in the following question: is it possible to set up arbitrary-orders SIR-type models with precise mathematical and biological basis like that of the original construction did by Kermack and McKendrick? What features of the models are maintained simply exchanging orders? Does the change in the order of derivatives automatically establish consistent models, regarding the parameters' definition, physical meaning, conservation, and units? What about non-negativity, monotonicity, among other issues? The use of techniques to solve arbitrary-order models analytically or numerically is an interesting field in itself. However, it is important to try to verify how, where, and why the non-integer derivatives interfere in the system.

In this context, a fractional model can be obtained through power-laws time-since-infection dependence in the infectiousness and removal functions. Thus, in [3] we followed the footsteps of Angstmann, Henry and McGann [1], where they use the probabilistic language of Continuous Time Random Walks (CTRW). The Riemann-Liouville derivative appears throughout the construction. We revisited the authors' work and built L1-scheme based discretization to the model, using optimization to apply it to the data of COVID-19. Here, we used this base to analyze other features, as non-negativity, monotonicity, reproduction number and equilibrium points, at Section 3, after that preliminary section. With MATLAB implementation, we discuss numerical features at Section 4.

2 Preliminary

In this section, we present the main definitions and results used in the work.

2.1 The Fractional Calculus

Arbitrary-Order Calculus, commonly known as Fractional Calculus, has been shown to be a very useful tool in capturing the dynamics of the physical process of several scientific objects, being generally related to the "memory effect". It was born in 1695, when l'Hôpital asked Leibniz about the meaning of a derivative of order

$1/2$. Over the next three centuries, important advances were made by Liouville, Riemann, Grünwald, Caputo and many others. However, it was only after the first International Conference on Fractional Calculus and Applications, in 1974, that the number of researchers in Fractional Calculus showed great growth, and even new formulations were proposed. Currently, congresses and symposia take place more frequently, with the *First Online Conference on Modern Fractional Calculus and its Applications (OCMFCA)* being held in 2020. The reader may refer to the reference [4] for a summarized chronology of publications in Fractional Calculus from 1695 to 2019, as well as for general results.

Below we consider $[a, b]$ a finite real interval and α a real number such that $0 \leq n - 1 < \alpha < n$, with n integer.

Definition 1: Riemann-Liouville integral in finite intervals. The Riemann-Liouville integral of an arbitrary order α is set to $t \in [a, b]$ by:

$$I^{\alpha}_{a+} f(t) = \frac{1}{\Gamma(\alpha)} \int_a^t (t - \theta)^{\alpha-1} f(\theta) d\theta. \tag{1}$$

After introducing the arbitrary-order integral, it is natural to search for the definition of the correspondent derivative.

Definition 2: Riemann-Liouville derivative at finite intervals. The Riemann-Liouville derivative of an arbitrary order α is set to $t \in [a, b]$ by:

$$D^{\alpha}_{a+} f(t) = D^n [I^{n-\alpha}_{a+} f(t)] = \frac{1}{\Gamma(n - \alpha)} \left(\frac{d^n}{dt^n}\right) \int_a^t (t - \theta)^{n-\alpha-1} f(\theta) d\theta \,, \tag{2}$$

with D^n representing the integer-order derivative.

We also present the definition of Caputo, for which, among other features, the derivative of a constant is zero:

Definition 3: Caputo derivative at finite intervals. The Caputo derivative of an arbitrary order α is set to $t \in [a, b]$ by:

$${}^{C}D^{\alpha}_{a+} f(t) = I^{n-\alpha}_{a+} [D^n f(t)] = \frac{1}{\Gamma(n - \alpha)} \int_a^t (t - \theta)^{n-\alpha-1} \frac{d^n}{d\theta^n} f(\theta) d\theta \,. \tag{3}$$

Finally, we present the Mittag-Leffler functions with one, two and three parameters. The classic Mittag-Leffler function with one parameter can be considered a generalization of the exponential function. Due to its importance in solving several arbitrary-order differential equations, it was nicknamed "queen of special functions" of the Fractional Calculus. Its importance for Fractional Calculus resembles the importance of the exponential function for classical calculus. We present the following definition [4]:

Definition 4: Mittag-Leffler function with one, two and three parameters. Let z be a complex number and three parameters α, β complex and ρ real such that $Re(\alpha) > 0, Re(\beta) > 0, \rho > 0$. We define the Mittag-Leffler function with three parameters through the power series

$$E^{\rho}_{\alpha,\beta}(z) = \sum_{k=0}^{\infty} \frac{(\rho)_k}{\Gamma(\alpha k + \beta)} \frac{z^k}{k!}, \tag{4}$$

where $(\rho)_k$ is the Pochhammer symbol, defined by

$$(\rho)_k = \frac{\Gamma(\rho + k)}{\Gamma(\rho)}. \tag{5}$$

Particularly, when $\rho = 1$, we have $(\rho)_k = k!$ and the two-parameter Mittag–Leffler function, denoted simply by $E^1_{\alpha,\beta}(t) = E_{\alpha,\beta}(t)$. When $\rho = \beta = 1$, we obtain the Mittag-Leffler function with one parameter, denoted by $E^1_{\alpha,1}(t) = E_{\alpha,1}(t) = E_{\alpha}(t)$. We point out that this function generalizes the exponential function, being equal to it when $\alpha = \beta = \rho = 1$.

2.2 The SIR Model

In 1927, the SIR (Susceptible-Infected-Removed) model was notably introduced by McKendrick and Kermack [5]. The mathematical formalism that carefully underpinned the construction of this epidemiological model is, unfortunately, not widespread, with the model being presented, in general, summarized in Figure 1.

In the diagram, $S(t)$ is the number of susceptibles, $I(t)$ the number of currently infected and $R(t)$ the number of removed, by recovery or death, at time t. The population $N = S(t) + I(t) + R(t)$ is constant and it is assumed that recovered are immune during the period under analysis. We also ignore the latency period of the disease.

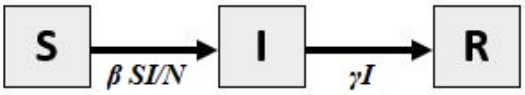

Figure 1. SIR model flow diagram without vital dynamics.

$$S'(t) = -\beta S(t)I(t)/N, \quad (6)$$

$$I'(t) = \beta S(t)I(t)/N - \gamma I(t), \quad (7)$$

$$R'(t) = \gamma I(t). \quad (8)$$

The model is written in eq. (6)-eq. (8), where β is the transmission coefficient, related, for instance, to the number of contacts of an individual and to the probability that a contact will result in contagion, and γ is the rate at which individuals move from the infectious compartment to the removed compartment, both with unit [time]$^{-1}$. The constant $1/\gamma$ is the average time in which an individual is infectious.

Also, throughout the development of the mathematical epidemiology, the so-called reproduction number $\Re$ plays an important role, reflecting how infectious a disease is in a given context, while the basic reproduction number, $\Re_0$, is the reproduction number when there is no immunity or intervention in the transmission of the disease. Under classic conditions, $\Re$ is defined as the average number of infections that a single individual can generate during the infectious period [6]. The $\Re_0$ represents this number at the start of infection, that is, the average number of infections that an individual can generate after being introduced into a fully susceptible population.

In traditional models, epidemics cannot occur when $\Re_0$ is less than 1 and established outbreaks will disappear if interventions or the depletion of the susceptible part of the population are sufficient to keep $\Re$ below 1. In simple models, like the classic SIR, we have $\Re(t) = \Re_0 S(t)/N$. Thus, the behavior of the infection is almost completely determined by the $\Re_0$, whose value determines not only the change in the stability of the disease-free equilibrium, but also when the endemic equilibrium becomes possible [6].

3 Arbitrary-order SIR model constructed with Mittag-Leffler distribution

So far, we have not been able to find a physical set up that allows to change the orders of the classical derivatives, even if the units are corrected and the new orders are the same in all of the compartments. We hold discussions in this regard in [7]. As said, we believe that the appearance of arbitrary-order derivatives can be obtained through potential laws in the infectivity and removal functions. Thus, we present in the article [3] a physical derivation of an arbitrary-order model, following the steps of Angstmann, Henry and McGann [8], using the probabilistic language of the Continuous Time Random Walks (CTRW). The individual's removal time from the infectious compartment follows a Mittag-Leffler distribution related to α, while the parameter β is related to the law of the infectivity function. The Riemann-Liouville derivative appears throughout the set up and the arbitrary-order SIR model with $1 \geq \beta \geq \alpha > 0$ is given by

$$\frac{dS(t)}{dt} = \gamma(t)N - \frac{\omega(t)S(t)\theta(t,0)}{N\tau^\beta} D^{1-\beta}\left(\frac{I(t)}{\theta(t,0)}\right) - \gamma(t)S(t), \quad (9)$$

$$\frac{dI(t)}{dt} = \frac{\omega(t)S(t)\theta(t,0)}{N\tau^\beta} D^{1-\beta}\left(\frac{I(t)}{\theta(t,0)}\right) - \frac{\theta(t,0)}{\tau^\alpha} D^{1-\alpha}\left(\frac{I(t)}{\theta(t,0)}\right) - \gamma(t)I(t), \quad (10)$$

$$\frac{dR(t)}{dt} = \frac{\theta(t,0)}{\tau^\alpha} D^{1-\alpha}\left(\frac{I(t)}{\theta(t,0)}\right) - \gamma(t)R(t), \quad (11)$$

where $\gamma(t)$ is the vital dynamic; $\omega(t)$, the extrinsic infectivity; N, the total population; τ, a scale parameter and, $\theta(t,t')$, the probability that an infectious since t' has not died of natural death until t. Note that $dN(t)/dt = dS(t)/dt + dI(t)/dt + dR(t)/dt = 0$, so the population remains constant. If $\beta = \alpha = 1$ and $\gamma(t) \equiv \gamma$, $\omega(t) \equiv \omega$ are considered constants, we get the traditional SIR model. We consider $1 \geq \beta \geq \alpha > 0$ for some reasons: first, because α and β came from Mittag-Leffler functions for infectivity and survival, being considered positive as in most definitions. Furthermore, to ensure that the intrinsic infectivity function is positive, we use complete monotonicity, which is guaranteed if α is not greater than 1 and than β. Finally, we use $\beta \leq 1$ because then we ensure that the infectivity function is non-increasing. We highlight that the units are balanced by construction, because $\omega(t)$ and $\theta(t,0)$ are dimensionless, while τ has dimension [time].

In [3], we revisited the authors' work and, in addition to starting the discussion of the reproduction number of their model, we used optimization to apply the model to data from the Brazilian and Italian COVID-19 pandemic, while in [9] we deal with pandemic data in Brazilian states. Also, in [10] we did parameter analysis in the model eq. (9)-eq. (11), improving biological interpretation of the parameters. Particularly, decreasing α, the tail of the survival function (independent of vital dynamics) becomes heavier. On the other hand, increasing β makes the intrinsic infectivity lower in the beginning, but higher with time.

3.1 Non-negativity and Monotonicity

We present the following result:

Proposition 1. Assuming that the solution of the system eq. (9)-eq. (11) exists and is unique, with initial conditions $S(0) > 0, I(0) > 0$ and $R(0) = N - S(0) - I(0) \geq 0$, the functions $S(t), I(t), R(t), D^{1-\beta}(I(t)/\theta(t,0))$ and $D^{1-\alpha}(I(t)/\theta(t,0))$ are non-negative for $t > 0$. Furthermore, $S(t), I(t), R(t) \leq N$ for all t.

The proof for the case without vital dynamics follows as in classic cases. With vital dynamics, we must use the positivity of the functions involved on construction. It will be explicit in future work. The next proposition is a consequence:

Proposition 2. If the system eq. (9)-eq. (11) has no vital dynamics, that is, $\gamma(t) \equiv 0$, then $S(t)$ and $R(t)$ are monotone decreasing and increasing, respectively.

3.2 Reproduction number

The effective reproduction number at time t' can be understood as the expected number of individuals that will be infected by an infectious individual since t. We can calculate, as in [3],

$$\Re(t') = \int_{t'}^{\infty} \frac{S(t)}{N\tau^{\beta}} \omega(t)\theta(t,t')(t-t')^{\beta-1} E_{\alpha,\beta}\left(-\left(\frac{(t-t')}{\tau}\right)^{\alpha}\right) dt. \tag{12}$$

Therefore, if we take $\gamma(t) \equiv \gamma > 0$ and disregard the variation of $S(t)$, by definition or simply considering that $S(t) \approx S(t')$ during the individual's infectious period, we can simplify the result by removing the $S(t)$ from the integral. Considering $S(0) \approx N$, for the constant $\omega(t) \equiv \omega$ case we have:

$$\Re_0 = \frac{\omega\gamma^{\alpha-\beta}}{\tau^{\beta}\gamma^{\alpha} + \tau^{\beta-\alpha}}; \qquad \Re(t') = \frac{S(t')\omega}{N\tau^{\beta}} \frac{\gamma^{\alpha-\beta}}{\gamma^{\alpha} + \tau^{-\alpha}} = \Re_0 \cdot \frac{S(t')}{N}. \tag{13}$$

Here we point out that disregarding the variation of the $S(t)$ during the individual's infectious period is not an irrelevant choice: this assumption makes a big difference in the calculations. Thus, we will also use what we call the reproduction number S-variable $\Re^S(t')$, defined by the integral of eq. (12) without the approximation $S(t) \approx S(t')$. In that case,

$$\Re_0^S = \int_0^{\infty} \frac{S(t)}{N\tau^{\beta}} \omega(t) e^{-\gamma t} t^{\beta-1} E_{\alpha,\beta}\left(-\left(\frac{t}{\tau}\right)^{\alpha}\right) dt. \tag{14}$$

It is interesting to note that, in general, the peak of infected no longer occurs when $\Re(t') = 1$, nor when $\Re^S(t') = 1$. This also represents a difficulty in models of arbitrary orders or variable coefficients.

3.3 Equilibrium points

Following [8] and assuming that $\gamma(t) \equiv \gamma$ and $\lim_{t\to\infty} \omega(t) = \omega^*$ (possibly, $\omega^* = 0$), we can obtain a disease-free state:

$$S^* = N, \quad I^* = 0, \quad R^* = 0, \tag{15}$$

and, in the case where $\omega^* > 0$, also an endemic state:

$$S^* = \frac{((\tau\gamma)^{-\alpha} + 1)N}{\omega^*(\tau\gamma)^{-\beta}}, I^* = \frac{N}{(\tau\gamma)^{-\alpha} + 1} - \frac{N}{\omega^*(\tau\gamma)^{-\beta}}, R^* = \frac{N}{1 + (\tau\gamma)^{\alpha}} - \frac{N}{\omega^*(\tau\gamma)^{\alpha-\beta}}. \tag{16}$$

When $\omega(t) \equiv \omega$, we have $\omega^* = \omega$ and reconstruct the endemic state of the original article [8]. We observe that the endemic state makes physical sense only if we can have $I^* > 0$ and $R^* > 0$, that is, if

$$\omega^* > (\tau\gamma)^{\beta-\alpha} + (\tau\gamma)^{\beta}. \tag{17}$$

Remark 1. If $\omega \equiv \omega^*$, the eq. (17) criterion for the viability of the endemic state can be rewritten as $\Re_0 > 1$. Furthermore, the value S^* of the endemic state given in eq. (16) is on the form $S^* = N/\Re_0$. So, the $\Re_0$ has an essential relationship with the final size of the infection, as expected.

Thus, we have shown that if there are asymptotically stable equilibrium for the case $\gamma > 0$, then they are given by eq. (15)-eq. (16). However, we have not really proved that the defined states are asymptotically stable

equilibrium. We expect that the disease-free state be an asymptotically stable equilibrium when $\omega^* < (\tau\gamma)^{\beta-\alpha} + (\tau\gamma)^{\beta}$, while the endemic state must be asymptotically stable if $\omega^* > (\tau\gamma)^{\beta-\alpha} + (\tau\gamma)^{\beta}$.

For the case without vital dynamics, that is, $\gamma = 0$, if $\alpha = \beta$ and $\omega(t) \equiv \omega$, we can write $dS/dR = -(\omega S(t)/N)$. This is similar to the classic model, also discussed in [3]. Thus, the equilibrium point is the same as in the original case, namely, we have the following Theorem:

Theorem 1. If $\omega(t) \equiv \omega$, $\gamma = 0$, $i_0 > 0$ and $\alpha = \beta$ in the system eq. (9)-eq. (11), then the solution asymptotically approaches equilibrium $(S, I, R)_\infty$, where

$$R_\infty = N + \frac{N}{\omega} W_0\left(\frac{-S_0\omega e^{-\omega}}{N}\right), \tag{18}$$

and

$$S_\infty = S_0 \exp\left(-\frac{\omega}{N}R_\infty\right) = -\frac{N}{\omega}W_0\left(\frac{-S_0\omega e^{-\omega}}{N}\right), \qquad I_\infty = N - S_\infty - R_\infty = 0. \tag{19}$$

As in the classic case, if the disease is at the beginning, $S_0 \approx N$ and the epidemic does not occur if $\Re_0 = \omega < 1$.

If $\alpha \neq \beta$, we were unable to proceed with the equilibrium analysis, but the simulations seem to show that, in this case, $\lim_{t\to\infty} S(t) = 0$.

For the case with $\gamma > 0$, there are difficulties for the formal analysis of stability. However, following the ideas of Hethcote and Tudor [11], we provide the next Theorems. Explicit proofs will be accessible in future works.

Theorem 2. If $\omega(t)$ is limited with $\lim_{t\to\infty} \omega(t) = \omega^*$, $\gamma(t) \equiv \gamma$ and $\beta = 1$ in the system eq. (9)-eq. (11), then the disease-free equilibrium given by eq. (15) is globally asymptotically stable if $\omega^* < (\tau\gamma)^{1-\alpha} + (\tau\gamma)$.

Theorem 3. If $\gamma(t) \equiv \gamma, \omega(t) \equiv \omega$ are taken constant and $\beta = 1$ in the system eq. (9)-eq. (11), then the endemic state given by eq. (16) is locally asymptotically stable whenever feasible, ie when $\omega > (\tau\gamma)^{1-\alpha} + (\tau\gamma)$.

4 Numerical results

We set up a $L1$-scheme [12] based discretization for the arbitrary-order SIR model eq. (9)-eq. (11). In the Figures 2-5, we consider $N = 1000000$, time step $dt = 0.1$ and initial conditions $I(0) = 1$, $S(0) = N - 1$ and $R(0) = 0$. In Figure 2, we illustrate the Proposition 2, which guarantees the monotonicity of the S and R compartments without vital dynamics. In the Figure 3, we illustrate the Theorem 1. We emphasize that, for $\beta \neq \alpha$, it seems to occur $\lim_{t\to\infty} S(t) = 0$. Now, in Figure 4, we indicate the behaviour when $\Re_0 < 1$, showing the free-equilibrium given in Theorem 2. So, in Figure 5, we illustrate the equilibrium given in Theorem 3. We remark that, for this simulation, $\Re_0 \approx 12.6$, $\Re_0^S \approx 5.8$, $\Re_{pico} \approx 2.3$ and $\Re_{pico}^S \approx 0.9$. We note that $\Re_{pico}^S < 1$ seems to us more realistic, because each person would be infecting less than one person, so the disease would be dying out. Next, in Figures 6-7, we consider an exponential decay in value over time, $\omega(t) = \omega \cdot e^{-t/100}$. Thus, $\omega^* = 0$ and there is only the disease-free equilibrium, ie, the trajectory returns to $(N, 0, 0)$.

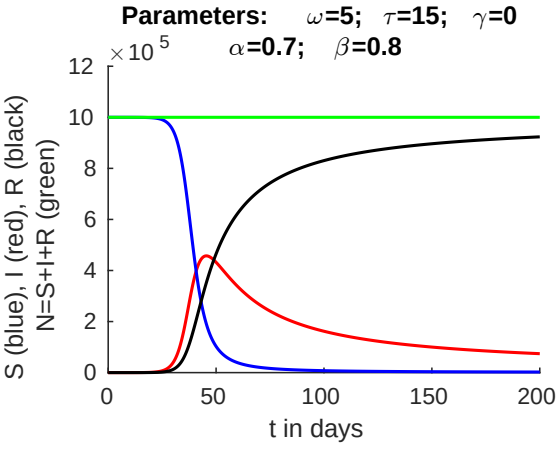

Figure 2. Monotonicity of S and R.

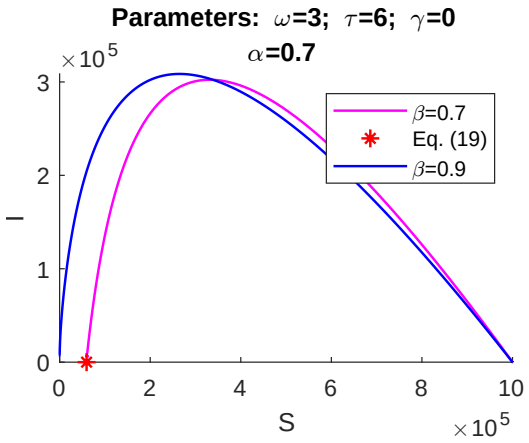

Figure 3. Equilibrium without dynamic.

Finally, in Figures 8-9, we illustrate the result of optimization to real data of COVID-19 based in [3]. According to the available data of the COVID-19 pandemic on Brazil, we apply through MATLAB the Least Squares Method using the FDIPA [13] algorithm to minimize the function $f(\omega, \tau) = ||AI - I||^2 + ||AR - R||^2$,

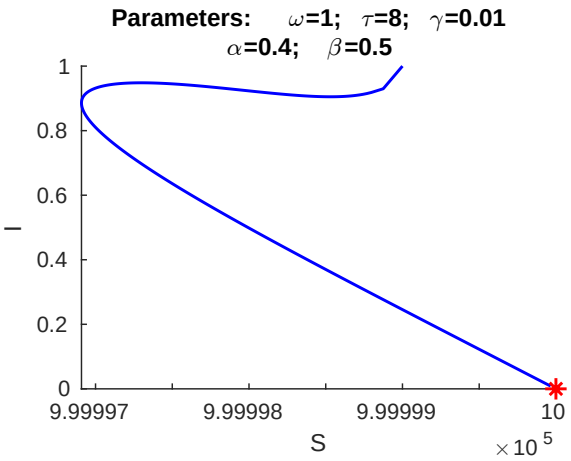

Figure 4. Equilibrium for $\Re_0 < 1$.

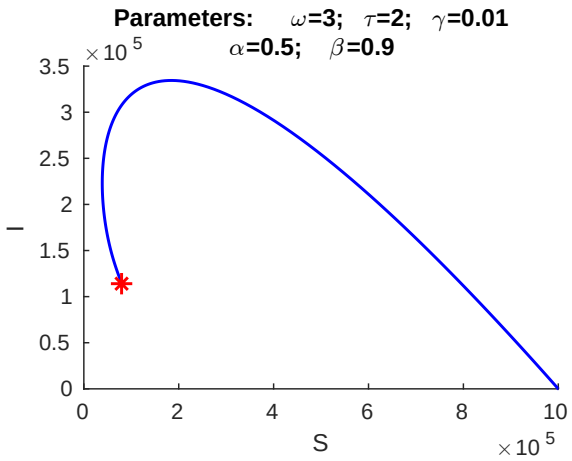

Figure 5. Equilibrium for $\Re_0 > 1$.

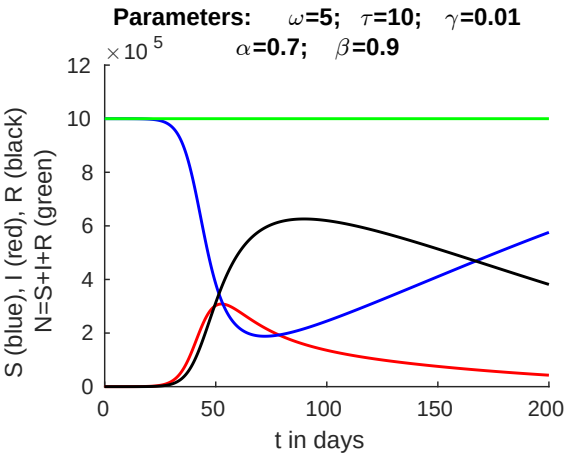

Figure 6. Case $\omega^* = 0$.

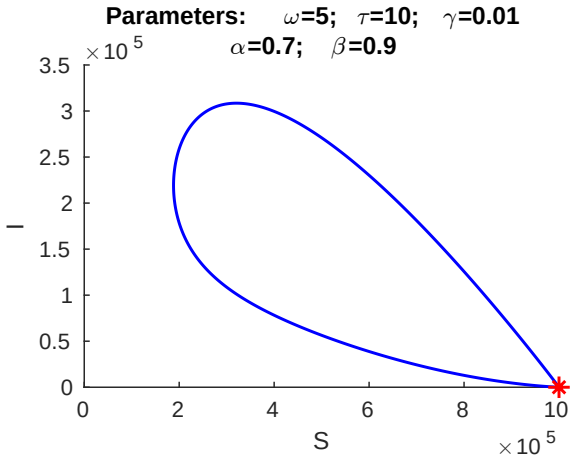

Figure 7. Equilibrium for $\omega^* = 0$.

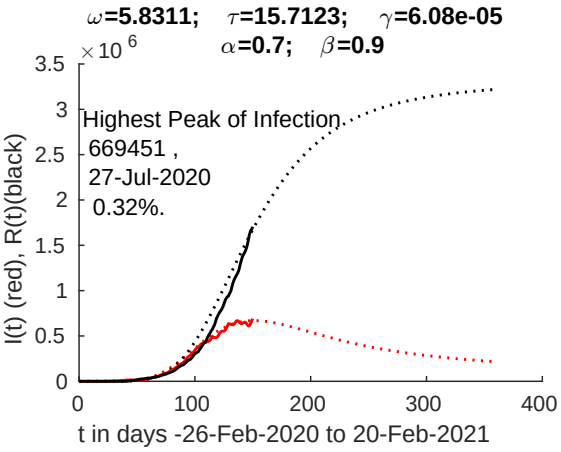

Figure 8. Projection of first wave.

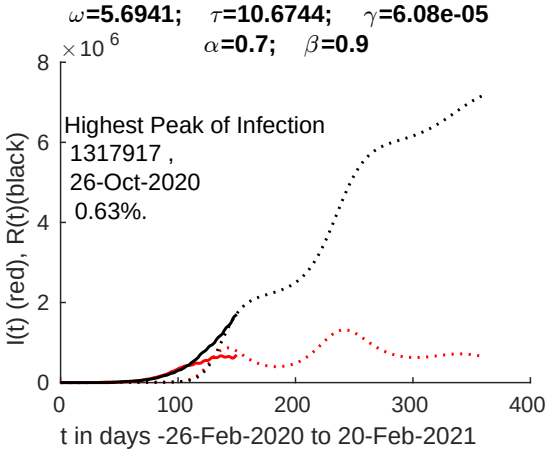

Figure 9. Oscillatory projection.

where AI is the data of the active infected and, AR, the data of those removed. We used $N = 210147125$ and $S(0) = N - 1, I(0) = 1, R(0) = 0$. In Figure 8, we consider $\omega(t) = \omega \cdot e^{-t/a}$, with $a = 70$. The dotted lines are the result of the model, while the solid lines are the real data from February 26 to July 25 of 2020. We realize, from the current viewpoint, that this simulation could fit well the first wave of Brazilian pandemic. In Figure 9, we use an exponential decay with oscillations, representing relaxation and periodic hardening of the containment measures: $\omega(t) = \omega \cdot e^{-t/a} \cdot \cos^2(t\pi/b)$, with $a = 140$ and $b = 110$. The graphic shown is a small adaptation of Figure 12 of the article [3] and provides, in the period under analysis, three waves, the second being the largest. The similarity between the graphic and what happened in Brazil drives us to continue studying oscillatory models.

5 Conclusions

We re-present a meaningful arbitrary-order SIR model from [3], intending to complete previous results. We present the non-negativity result and, without vital dynamics, the monotonicity result, which is in agreement with expectations. Were also shown the reproduction numbers and we present a new proposal for their approximation.

So, it was shown that, in the case without vital dynamics, the equilibrium when $\alpha = \beta$ is the same as in the classic case. We hypothesize that, for $\alpha \neq \beta$, we have $\lim_{t\to\infty} S(t) = 0$. Then, we present the equilibrium points for the case with vital dynamics.

Results in MATLAB corroborate the theoretical results. Also, the application of the model to COVID-19 via Least Squares using the FDIPA was presented. The results built using only the data up to July 2020 proved to be interesting from the current viewpoint, with regard to the first wave modeling and also to the model with oscillatory infectivity. Thus, we believe that, with more accurate data, the model can be really useful in analyzing epidemics.

Future work intends explicit the proofs of the results, as well as prove the raised hypotheses and bring a more exhaustive analysis of the model and reproduction numbers. Also, we are leading, for next works, investigations on the different waves of pandemic, with oscillatory models or considering each wave separately.

Acknowledgements. We appreciate the support of the Coordenação de Aperfeiçoamento de Pessoal de Nível Superior - Brasil (CAPES) - Financing Code 001.

Authorship statement. The authors hereby confirm that they are the sole liable persons responsible for the authorship of this work, and that all material that has been herein included as part of the present paper is either the property (and authorship) of the authors, or has the permission of the owners to be included here.

References

[1] L. Cardoso, F. Dos Santos, and R. Camargo. Analysis of fractional-order models for hepatitis b. *Computational and Applied Mathematics*, vol. 37, n. 4, pp. 4570–4586, 2018.

[2] J. P. C. d. Santos, E. Monteiro, and G. B. Vieira. Global stability of fractional sir epidemic model. *Proceeding Series of the Brazilian Society of Computational and Applied Mathematics*, vol. 5, n. 1, 2017.

[3] N. Monteiro and S. Mazorche. Fractional derivatives applied to epidemiology. *Trends in Computational and Applied Mathematics*, vol. 0, n. 0, pp. 157–177, 2021a.

[4] E. C. d. Oliveira. *Solved Exercises in Fractional Calculus*. Springer, 2019.

[5] W. O. Kermack and A. G. McKendrick. Contributions to the mathematical theory of epidemics–i. 1927., 1991.

[6] H. W. Hethcote. The mathematics of infectious diseases. *SIAM review*, vol. 42, n. 4, pp. 599–653, 2000.

[7] N. Monteiro and S. Mazorche. Modelos epidemiológicos fracionários: o que se perde, o que se ganha, o que se transforma? In *Proceeding Series of the Brazilian Society of Computational and Applied Mathematics (CNMAC)*, pp. (to appear), 2021b.

[8] C. N. Angstmann, B. I. Henry, and A. V. McGann. A fractional-order infectivity and recovery sir model. *Fractal and Fractional*, vol. 1, n. 1, pp. 11, 2017.

[9] N. Monteiro and S. Mazorche. Application of a fractional sir model built with mittag-leffler distribution. In *Mathematical Congress of the Americas. Poster presentation*, 2021c.

[10] N. Monteiro and S. Mazorche. Estudo de um modelo sir fracionário construído com distribuição de mittag-leffler. In *Proceeding Series of the Brazilian Society of Computational and Applied Mathematics (CNMAC). Poster presentation*, pp. (to appear), 2021d.

[11] H. W. Hethcote and D. W. Tudor. Integral equation models for endemic infectious diseases. *Journal of mathematical biology*, vol. 9, n. 1, pp. 37–47, 1980.

[12] K. Oldham and J. Spanier. *The fractional calculus theory and applications of differentiation and integration to arbitrary order*. Elsevier, 1974.

[13] J. Herskovits. Feasible direction interior-point technique for nonlinear optimization. *Journal of optimization theory and applications*, vol. 99, n. 1, pp. 121–146, 1998.